Prediction of total silicon concentrations in French soils using pedotransferfunctions from mid-infrared spectrum and pedological attributes

Amélia Landre, Nicolas Saby, Bernard Barthès, Céline Ratié, A Guerin, A. Etayo, Budiman Minasny, Marion Bardy, Jean-Dominique Meunier, Sophie Cornu

Prediction of total silicon concentrations in French soils using pedotransfer functions from mid-infrared spectrum and pedological attributes

Co-authors: Landré, A.[a], Saby, N.P.A.[a], Barthès, B.G.[b], Ratié C.[a], Guerin, A.[c] Etayo, A.[c], Minasny, B.[d], Bardy, M.[a], Meunier, J.-D.[e], Cornu, S.[e]

a) INRA, Infosol, US 1106, Orléans, France
b) IRD, UMR Eco&Sols, Montpellier SupAgro, 2 place Viala, 34060 Montpellier Cedex 2, France
c) INRA, Laboratoire d'Analyses des Sols US, Arras, France
d) School of Life and Environmental Sciences and Sydney Institute of Agriculture, The University of Sydney, NSW 2006, Australia
e) Aix-Marseille Univ, CNRS, IRD, Coll de France, INRA, CEREGE, Aix-en-Provence, France

Abstract

Silicon (Si) is the second most abundant element of the Earth's crust, and its terrestrial cycle depends on soil, vegetation, and human activities. The spatial extent of terrestrial Si perturbation is poorly documented since maps of Si concentration in soils are rare. In addition, Si content is rarely measured in non-paddy soil databases. Here we demonstrate that pedotransfer functions based on either pedological attributes (particle size fraction, pH, organic carbon, cation exchange capacity, calcium carbonate and parent material) or mid infrared spectra (MIRS) can be used to accurately predict total Si concentration. In this

research, we utilised a unique dataset from the French monitoring network of soil quality (RMQS - Réseau de Mesures de la Qualité des Sols) database. Pedotransfer functions were built using a regression tree model on a subset of the data for which total Si concentration was measured. To compare the relative performance of the models obtained for the two different sources of data, a suite of performance indicators were calculated. Our results showed that PTF based on MIR spectra produces highly accurate and precise estimates of the total Si concentration for French soils. The pedological PTF is less accurate, but still provides a good estimation of the Si concentration. The pedological PTF provides an alternative method when only basic soil data are available, and an approximate estimation of Si concentrations is sufficient. These PTFs can be readily applied at the European scale except on a few soil groups not represented in France.

keywords

Silicon, silica, pedotransfer function, diffuse reflectance, FTIR, mid-infrared spectra, regression tree, soil mointoring.

1- Introduction

Silicon (Si) is the second most abundant element of the Earth's crust, after oxygen, with an average mass concentration of 28% (Wedepohl, 1995). The SiO_4 tetrahedron is the elemental brick of soil minerals which constitutes the basic structure of Si in nature from solid (silicates) to soluble (silicic acid) states. Through weathering of primary minerals, Si is released into soil solution where it is either recombined with other elements to form secondary minerals, adsorbed on oxides surfaces, absorbed by plants or exported to groundwater and rivers. Indeed, despite being considered as a non-essential element, Si is encountered in most terrestrial plants with concentrations highly variable, ranging from less than 0.2 to more than 10 % dry weight (Ma and Takahashi, 2002). Meanwhile, plant Si is a significant pool of the global Si cycle as evidenced from the total annual biogenic Si retention in terrestrial plants, which is estimated in the same order of magnitude as the Si fixed annually by diatoms in the ocean (Carey and Fulweiler, 2012; Loucaides et al., 2010). The terrestrial Si cycle notably depends on the type of vegetation (Alexandre et al., 1997; Bartoli, 1983; Blecker et al., 2006; Cornelis et al., 2010) and is suggested to be perturbed by human activities through urban activities, agriculture and deforestation (Conley et al., 2008; Struyf et al., 2010; Vandevenne et al., 2012). However, the extent of this perturbation is not well documented. One approach to address this question is a spatial analysis at the territory scale. Soil Si maps are rare to our knowledge, with the notable exception of the Si map for European soils with one site every 2500 km² (De Vos et al., 2006; Reimann et al., 2014). Soil silica content is mostly measured in rice-growing areas (Minasny et al., 2016), but rarely measured in non-paddy soil databases, especially in most of the national soil monitoring networks of Europe (Arrouays et al., 2008; Imrie et al., 2008; Morvan et al., 2008). The possible reasons are (1) the cost of the measurement and (2) little attention paid to Si in soil and agriculture until now.

63 In the literature, several soil characteristics, generally hydraulic properties or bulk density,
64 (Baldwin et al., 2017; Van Looy et al., 2017; Wösten et al., 1999), among others), have been
65 estimated by predictive functions based on pedological characteristics (organic matter,
66 particle size distribution etc.). This is commonly known as pedotransfer function (PTFs).
67 Recently, infrared spectroscopy has been proposed as a rapid and cost-effective alternative of
68 conventional chemical analysis as one spectrum can be used to derive several soil parameters
69 (Bertrand et al., 2002; Janik et al., 1998; McCarty et al., 2002; Minasny et al., 2009; Soriano-
70 Disla et al., 2014, 2013; Viscarra Rossel et al., 2006). In their review, Viscarra Rossel et al.
71 (2006) demonstrated mid infrared spectra (MIRS) produce better accuracy over near infrared
72 spectra (NIRS) for a large number of soils properties. However, that review did not show any
73 study that predicts Si from infrared spectra. Nevertheless, Janik et al. (1995) showed that soils
74 dominated by quartz, which is made up of SiO_2, has a peak around 1700-2000 cm^{-1}. Other
75 studies showed that MIRS presented good predictions of oxalate extractable Si, a specific
76 form of Si used to assess the degree of soil weathering (Bertrand et al., 2002; Minasny et al.,
77 2009). These findings suggest that MIRS could be used for prediction of total Si as recently
78 demonstrated by Mohanty et al. (2016).
79 In this study, we developed and compared pedotransfer functions of total topsoil Si
80 concentrations based on either pedological data (particle size fraction, pH, organic carbon,
81 cation exchange capacity, calcium carbonate and parent material) or MIRS. These data were
82 derived from the French monitoring network of soil quality database, RMQS (Réseau de
83 Mesures de la Qualité des Sols (Arrouays et al., 2003; Jolivet et al., 2006). Pedotransfer
84 functions were built on the RMQS data subset on which total Si concentrations were
85 measured. Subsequently, the PTFs were applied to the whole RMQS dataset to predict topsoil
86 Si concentration for the whole of France.

2- Materials and methods

2.1- Soil samples

2.1.1- The RMQS database

The RMQS monitoring network encompasses 2088 sites sampled following a 16 × 16 km² regular grid across the French metropolitan territory (550 000km²). At each site, land-use, climate, soil type and parent material were described. Twenty five individual cores were sampled, from the topsoil (0-30 cm), using an unaligned sampling design within a 20 × 20 m area (Jolivet et al., 2006). Core samples were then bulked. The resulting composite samples were air-dried and sieved to 2 mm before analysis. Particle-size distribution, pH in water, organic carbon (OC), cation exchange capacity (CEC), calcium carbonate ($CaCO_3$) were analyzed according to international (ISO) or French (NF) standardized methods by the accredited Soil Analysis Laboratory of INRA (Arras, France) (Table 1). This study is based on the analytical results of the samples collected from 2002 to 2009 (first sampling campaign) for the previous characteristics.

2.1.2- MIRS data

MIRS were also acquired on RMQS samples (Grinand et al., 2012). 0.5-g aliquots of < 0.2-mm ground sample were scanned from 4000 to 400 cm^{-1} (i.e., 2500-25,000 nm) at 4 cm^{-1} resolution using a Nicolet 6700 Diffusive Reflectance Fourier Transform Spectrophotometer (Thermo Fisher Scientific Instruments, Madison, WI, USA). Then, 32 scans per sample were acquired and averaged. Spectra were recorded as absorbance.

MIRS were pre-processed, before statistical modelling to reduce baseline variations, enhance spectral features, reduce the particle-size scattering effect, remove linear or curvilinear trends of each spectrum, or remove additive or multiplicative signal effects (Boysworth and Booksh,

2008). The pre-processing routine consisted of an 11 bands window smoothing Savitzky–Golay filter (Savitzky and Golay, 1964) using the *sgolayfilt* function from the signal R package (Ligges et al., 2015) followed by a standard normal variate (SNV, Barnes et al., 1989) transform.

2.1.3- Selection of samples for total Si analysis

To develop the pedotransfer functions, a subset of 673 samples from the 2088 RMQS samples, called hereafter the Si dataset, were analyzed for total Si concentration. The subset sites were selected using the following criteria: (1) one site out of four from the original grid excluding Corsica, and (2) 160 sites randomly selected from the remaining sites (Figure 1). This sub-sampling of the grid preserves the systematic grid sampling. This gridsampling method was established by (Brus and Saby, 2016) as a flexible design for statistical soil surveys leading to relatively accurate estimates of the statistical distribution of spatial parameters. Total Si concentration was measured on air-dried, less than 2 mm samples by inductively coupled plasma atomic emission spectrometry (ICP-AES) after sodium peroxide fusion of the samples.

2.2- Total Si modelling and predictions

2.2.1- Pedotransfer functions (PTFs)

Pedotransfer functions predicting total Si content was established using two different types of soil variables as inputs:

(1) basic pedological attributes including particle size fraction, pH, organic carbon, cation exchange capacity, calcium carbonate and parent material, or

(2) pre-processed MIRS data,

These PTFs are termed as pedological PTF and MIRS PTF hereafter. The variables of the pedological PTF were chosen from the most common soil analytical variables in soil databases. For that reason, parent material was also included, while soil type was not as it had only a limited influence in the model (data not shown).

2.2.2- Statistical modelling approach

Regression procedure: Quantitative prediction of total Si concentrations by the soil properties and the MIRS were obtained using Cubist, a type of regression tree model (Quinlan, 1992). The Cubist model is a form of regression rules that build regression trees with final nodes containing linear models instead of discrete values. Cubist creates interpretable rules that describe the relationships between predictive variables (in this case spectral bands or soil properties) and the variable of interest (Si). Minasny et al. (2009) and Minasny and McBratney (2008) demonstrated that this approach could provide higher accuracy than the partial-least-squares (PLS) approach, commonly used in chemometrics. Moreover, this type of approach is flexible as it can handle both quantitative and qualitative variables as well as spectral data, which allows having a unique approach for both PTFs, and thus their results can be fairly compared.

To optimize the Cubist model, two parameters can be adjusted: the number of model trees as ensembles (*committees*) and the number of nearest–neighbors to adjust the prediction of the rules (*neighbors*). To optimize the model parameters, we used the *train* function in the caret R package. The tuning parameter 'neighbors' was held constant at a value of zero to avoid shortcomings in the interpretability of the rules by local averaging. The optimal numbers of 'committees' was found to be 5 for the two PTFs.

Calibration and evaluation steps: The modelling approach is summarized in Figure 2. we used a leave *p* out cross-validation approach combined with a bootstrap step (James et al., 2013). The *p* cross-validation leaves out a *p* proportion of samples for validation. We used a

75%-25% split for calibration and validation respectively, and this procedure was repeated 10 times. Cross-validation allows a more robust assessment of the quality of the prediction. The subdivision was performed using the conditioned Latin Hypercube Sampling (cLHS) method (Minasny and McBratney, 2006). This method is a stratified random procedure that provides an efficient way of sampling variables from their multivariate distributions. The bootstrap step involved simulating 100 datasets by random sampling with replacement from 95% of the calibration dataset (formed at the cross-validation step). This whole procedure generated 100 Cubist models in the calibration procedure. These outcomes were used to build the distribution of the prediction. The mean prediction could be obtained from the average of the 100 bootstrapped models.

Software: Our modelling approach involves a large number of model calibrations and parallel processing was used to handle the computational load. Parallel processing was implemented in R using the packages foreach (Calaway et al., 2017b) and doParrallel (Calaway et al., 2017a). All data analyses were performed using the R statistical environment (R core Team, 2017) for descriptive statistics, spectrum pre-processing and model building. We used the Cubist implementation from the Cubist package (Kuhn et al., 2016), the cLHS function implemented in clhs package (Roudier, 2011).

2.3- Assessments and interpretations

2.3.1- Representativeness assessment

Before evaluating the prediction ability of the two PTFs, we first checked that the Si dataset used to develop the PTFs was representative of the whole RMQS dataset. Graphical and numerical comparison of the statistical distribution of the basic pedological data, and the MIR spectra were performed. The Wilcoxon test for the quantitative soil attributes was also performed to compare the two datasets (the Si dataset and the RMQS database). In addition,

principal component analyses (PCA) was performed on the pedological attribute as well as the MIRS variables. Using the PCA, samples with or without Si measurements can be readily compared. The PCA allows comparison of the multivariate variables, while the distribution analyses only consider one soil variable at a time.

2.3.2- Accuracy assessment

To compare the relative performance of the models obtained for the two PTFs, three conventional performance indicators were calculated: the coefficient of determination (R^2), the root mean square error (RMSE, also known as standard error of prediction, SEP) and the bias, which is the mean residual of the model. In addition, we took into account the probability distribution of model predictions using the continuous rank probability score average (CRPS, equation 6). The CRPS represents the closeness between the prediction distribution and the corresponding observations (Gneiting et al., 2007). This score is commonly used in meteorological forecasts as a verification tool for (probabilistic) forecast systems (Hersbach, 2000; Trinh et al., 2013). The metric is calculated using:

$$CRPS = \int_{-\infty}^{\infty} BS(y)\, dy\,, \qquad (6)$$

$$BS(y) = \frac{1}{n}\sum_{i=1}^{n} \{(F_i(y) - \mathbb{1}\,(x_i \leq y)\}^2\,, \qquad (7)$$

where $BS(y)$ denotes the Brier score (Brier, 1950) for probability forecasts of the binary event at the threshold value $y \in \mathbb{R}$, x is the observation and y is the model prediction, n the number of samples, F is the cumulative distribution function (CDF) of X, a random variable, such as $F(y) = P[X \leq y]$ and $\mathbb{1}$ is the Heaviside step function. This function is a discontinuous function where the value is zero for negative argument and unity for positive argument.

The CRPS is a distance criterion, which is a positive value and should be close to 0. The prediction is expressed in terms of a probability distribution rather than a single value. The

CRPS compares the cumulative probability distribution of the predicted value to the observed value. In our case, we only took into account the uncertainty of the prediction and assumed the uncertainty of the observation is small. The probability distribution of our observation is set to equal to 1 for the observed value and null elsewhere. As a distance, the CRPS can be linked to the mean absolute error used in the deterministic prediction. It uses the information provided by the probabilistic prediction instead of just using the mean of the median value. We used the crps function implemented in the verification package (Laboratory NCAR-Research Applications, 2015).

2.3.3- The importance of the predictors in the model

In order to interpret the PTFs results, we extracted and computed the variable of importance from the Cubist rulesets. The variable of importance is computed as the percentage of times each variable was used in a rule condition and/or a linear model. Following our calibration and validation step, we calculated the average importance of predictors over the 100 Cubist models produced by bootstrap and then over the 10 iterations of the cross-validation step for each PTF. Because it is an average value, the sum of the variables of importance do not sum up to 100.

3- Results & Discussion

3.1- Representativeness of the Si dataset compared to the whole RMQS dataset

Measured Si concentrations range from 22.81 to 455.8 g kg^{-1} over the Si dataset with a median equal to 327.2 g kg^{-1} (Figure 3). Soils with low total Si concentrations (under 124 g kg^{-1}, the statistical threshold for outliers in this dataset) were poorly represented (17 over 674; Figure 3). The corresponding samples originated from soils developed in sedimentary parent materials, mostly calcareous with a carbonate concentration of greater or equal to 395 g kg^{-1}.

The parent material distribution of both the Si dataset (n=673) and the RMQS set (n= 2088) are very similar (Figure 4). For the pedological attributes, the empirical density estimates of soil properties were well represented, both in the Si dataset and the RMQS (Figure 5). The summary statistics of the pedological attributes were reported in Table 2. The empirical density functions for both datasets overlapped. This is supported by the Wilcoxon test which showed no significant difference in the distribution for the considered attributes (p-values recorded in Table 2). Considering the whole dataset, the PCAs showed a good overlap between the RMQS sites with and without Si measurement (Figure 6). Therefore, we can consider the Si dataset to be representative of the whole RMQS.

3.2- Total Si prediction by the PTFs

The validation of the MIRS PTF estimating Si content was excellent with an R^2 of 0.96. Estimates from this PTF were unbiased, and their average RMSE is 15.31 g kg^{-1} (Table 3). The average CRPS was very close to the RMSE value. The validation of the pedological PTF

246 was also very good with an R^2 of 0.87. Estimates from the pedological PTF were slightly
247 biased, with an average RMSE of 26.48 g kg^{-1}. Finally, the average CRPS were larger
248 indicating higher prediction uncertainty. The results of leave *p* out cross-validation were also
249 used to compute indicators of the variability of the performance indicators (Table 3). The
250 standard deviation of these indicators for the MIRS PTF was small.
251 To better figure out the difference between the accuracy of the two PTFs, we plotted the
252 predicted *versus* measured Si concentrations for one iteration of the cross-validation steps
253 (Figure 7). For the MIRS PTF, the prediction and analytical uncertainties of the data are of the
254 same order of magnitude (Figure 7a) as suggested by the RMSE values. This means that this
255 PTF gives good predictions, and close to analytical measurements. In contrast, the pedological
256 PTF presents a larger prediction uncertainty than the MIRS PTF, and it also has larger
257 uncertainty compared to the analytical uncertainty (Figure 7b) as shown by RMSE results. In
258 addition, total Si concentration tends to be over-estimated by the pedological PTF at low
259 concentrations ($\leq$ 270 g kg^{-1}) and under-estimated at high concentrations ($\geq$ 370 g kg^{-1}). This
260 is further confirmed by the coefficients of the linear regression between observed and
261 predicted values of the pedological PTF, with 67.18 for the intercept and 0.80 for the slope. In
262 comparison, the MIRS PTF has an intercept of 22 g kg^{-1} and slope of 0.07. The bias maybe
263 due to the low representation in the dataset of samples having Si concentration lower than
264 12.5 %, as discussed earlier. The bias can also come from sites which were over predicted
265 where the Si concentrations are between 200 and 300 g kg^{-1}.
266 All in all, the MIRS PTF tends to show an accuracy as good as the chemical analysis when
267 considering both the prediction and analytical uncertainties. However, as predictions were
268 made on the basis of analytical measurements, the prediction uncertainty does not only come
269 from the model accuracy but also from the uncertainty of analytical measurements (Janik et
270 al., 1998). In our case, the analytical uncertainty was not taken into account in the prediction

uncertainty calculation, as they were not always available. Despite this, the obtained PTFs show an exceptional accuracy that is rarely obtained in the PTFs literature (Minasny et al., 2009; Viscarra Rossel et al., 2006). Viscarra Rossel et al. (2006) reported the accuracy of MIRS PTFs for different soil properties from the literature have R^2 values ranging from 0.07 to 0.98, where one third of the cases an R^2 value larger or equal to 0.90 was obtained. Minasny et al. (2009) built MIRS PTFs for predicting soil properties on three different databases and reported R^2 values from 0.0 for total S to 0.92 for CEC and OC. They concluded that basic soil organic and mineral constituents, as well as properties that are related to the mineral and organic components could be well predicted. This study confirms the hypothesis. PTFs based on pedological properties are generally used to predict hydrological properties that are difficult to measure (e.g., Baldwin et al., 2017; Wösten et al., 1999, among others) but seldom developed to predict chemical characteristics.

3.3- The Pedological significance of the calibrated PTFs

Regarding pedological significance, the MIRS PTF uses mostly combination-overtones bands of quartz ranging from 1800 to 2000 cm^{-1} (Table 4), to predict total Si concentration, which is expected, as quartz is a mineral composed of Si and oxygen (O) atoms (SiO_2) (Figure 8a). This region of the spectrum presents the peak with the most important weight (>80%) around 2000 cm^{-1} followed by two other peaks around 1800 and 1900 cm^{-1} (> 40%, Figure 8b, Table 4). The carbonate concentration also has a role in the MIRS PTF, with carbonates bands ranging from 2400 to 3100 cm^{-1}, which correspond to $CaCO_3$ bonds (Table 4). It exhibits three peaks of average weight > 20%, one around 2500 and two around 3000 cm^{-1} (Figure 8b). As shown in Figure 8a, samples with low Si concentration contain carbonates while samples with high Si concentration do not. This link is due to the absence of Si in carbonates (Table 4). Bands related to Si-O bond ranging from 1400 to 400 cm^{-1} also presents a noticeable weight in the PTF (Figure 8b).

For the pedological PTF, the two most important predictors are the organic carbon and the carbonate concentrations, with an average weight of 78.6% and 73.6% respectively. Carbonates as discussed for the MIRS PTF act as a diluent for Si, which is also the case of organic carbon. No significant organic carbon contribution was observed in the MIRS PTF probably because, in MIRS, "organic carbon cannot be identified with clearly separated peaks but as a whole spectral region with overlapping bands", as stated by Grinand et al. (2012). In the pedological PTF, an important influence of the sand fraction could be expected as a positive correlation between total Si and both fine and coarse sand is observed (Kendall's correlation coefficient: tau = 0.17 and p-value = $3.585\ 10^{-11}$; tau = 0.11 and p-value = $3.108\ 10^{-5}$, respectively). Indeed, these two variables have an average weight of 37% in the pedological PTF (Figure 9). In addition, the clay fraction also has an important weight in the pedological PTF (60%) with a negative correlation between the total Si concentration and the clay fraction (Kendall's correlation coefficient: tau = - 0.46 and p-value < 2.2e-16).

As a conclusion, the two PTFs were mainly underlined by the same processes: dilution of the Si concentration by carbonates, organic carbon and possibly the clay fraction to a lesser extent and concentration due to the presence of quartz mainly in the sand fractions.

3.4- Domain of potential application of the developed PTFs

We compared pedological PTF predictions of total Si concentration for the non-Si analysed RMQS sites to that predicted by the MIRS PTF (Figure 10). The relative difference of predictions between the two PTFs is small, 90% of the time, the difference between the 2 PTFS is less than 20%. This result highlights the consistency of the two PTFs and confirms that despite less accurate, the pedological PTF gives a reasonable estimation of the soil Si concentration for the whole dataset. The soil observations of this study came from a systematic probability sampling which leads to good spatial coverage, i.e. the sites are uniformly spread over France. This design proves to be efficient in providing accurate

estimates of means over the whole area and can be used to generalize the results for the whole area of France (Brus and Saby, 2016).

We further investigated if the domain of application of our PTFs at the European scale by comparing the Si concentrations statistical distribution of the Si measurements analytically measured from the RMQS to that of the Geochemical Mapping of Agricultural Soils (GEMAS) dataset (De Vos et al., 2006; Reimann et al., 2014). The GEMAS study provided a few soil Si data over the French territory with one site every 2500 km², i.e. 214 sites for France. Comparing those two distributions for France showed 1) a slight over-estimation of the occurrence of soils with concentrations around 300 g kg^{-1} ; 2) an under-estimation of soils with concentrations around 400 g kg^{-1} ; 3) a slight smaller median of the French soil Si concentrations (320.7 g kg^{-1}). Nevertheless, the Mann and Whitney test shows no significant difference between the two datasets (p-value = 0.5757). For the European territory, the comparison is shown in Figure 11. The two datasets cover the same range of Si concentration with an over-representation of the soils with Si concentration ranging from 350 to 400 g kg^{-1} in French compare to other European soils, resulting in contrasted median Si-concentrations of 327.2 g kg^{-1} and 313.9 g kg^{-1} respectively. When looking at the Si average, the Mann and Whitney test also shows a small significant difference between the two datasets ($0.05 > p\text{-value} = 0.02273 > 0.01$). This result was expected since France is one of the countries exhibiting the largest soil diversity in the world (Minasny et al., 2010). Thus, the established PTFs can be applied at the Europeans scale to predict total soil Si concentrations at a higher spatial density than that provided by the GEMAS study with the exception of some soil types that are not represented in France, such as Chernozems, Kasternozem, Solonetz.

Finally, to better define the application range of our PTFs outside of Europe, future users can determine the appropriate domain of application of a specific PTF to a new dataset using distance metrics, such as the one presented by Tranter et al. (2009).

4- Conclusions

We developed PTFs based on either MIRS or pedological data to estimate the topsoil total Si concentration. Both PTFs provide accurate estimations of the total Si concentration for French soils. These PTFs are underlined by the link between Si and quartz, organic matter, and carbonate contents. The PTF based on MIRS data produces a highly accurate and precise estimates. Since the acquisition of MIRS data allows the estimation of a range of soil properties, such as particle size fraction, major elements or chemical properties that are related to surface solid characteristics like CEC, the use of MIRS PTF represents a powerful tool for populating soil databases. The pedological PTF is less accurate, but still provides a reasonable estimation of the Si concentration for French soils. It is an alternative method when only pedological data are available and an approximate estimation of Si concentrations is sufficient. This PTF can be applied to databases of legacy soil data to provide an initial estimate of Si distribution.

Both PTFs can be readily applied at the European scale with the possible exclusion of a few soil groups not represented in France. For these soil types, this study provides a pathway for the development of new calibration PTFs procedure to local data.

This modelling approach yields very robust results with an adaptable method. Overall, this work provides the first approach to estimate nation-wide topsoil total Si concentration and opens the way for further works on Si in soils.

5- Acknowledgements

This work was performed in the frame of the French ANR BioSiSol project (ANR-14-CE01-0002). RMQS soil sampling and physico-chemical analyses were supported by the GIS Sol, which is a scientific group of interest on soils involving the French Ministry for ecology and sustainable development and Ministry of agriculture, the French National forest inventory (IFN), ADEME (Agence de l'environnement et de la maîtrise de l'énergie, which is a French government agency concerned with environmental protection and energy management), IRD (Institut de recherche pour le développement, which is a French public research organization dedicated to southern countries) and INRA (Institut national de la recherche agronomique, which is a French public research organization dedicated to agriculture s.l.). Claudy Jolivet is thanked for his strong involvement in the RMQS monitoring network. Manon Villeneuve, Emmanuel Bourdon, Didier Brunet, Jérôme Lourd, and Clément Robin (IRD) are thanked for their skillful technical assistance and strong investment in the tedious scanning process of the RMQS soil library.

6- References

Alexandre, A., Meunier, J.-D., Colin, F., Koud, J.-M., 1997. Plant impact on the biogeochemical cycle of silicon and related weathering processes. Geochim. Cosmochim. Acta 61, 677–682. https://doi.org/10.1016/S0016-7037(97)00001-X

Arrouays, D., Jolivet, C., Boulonne, L., Bodineau, G., Ratié, C., Saby, N., Grolleau, E., 2003. Le réseau de mesures de la qualité des sols (RMQS) de France. Etude Gest. Sols 10, 241.

Arrouays, D., Morvan, X., Saby, N., Richer de Forges, A., Le Bas, C., Bellamy, P.H., Üveges, B., Freudenschu\s s, A., Jones, A.R., Jones, R.J.A., others, 2008. Environmental Assessment of Soil for Monitoring. Volume IIa: Inventory & Monitoring. European Communities.

Baldwin, D., Manfreda, S., Keller, K., Smithwick, E.A.H., 2017. Predicting root zone soil moisture with soil properties and satellite near-surface moisture data across the conterminous United States. J. Hydrol. 546, 393–404. https://doi.org/10.1016/j.jhydrol.2017.01.020

Barnes, R.J., Dhanoa, M.S., Lister, S.J., 1989. Standard Normal Variate Transformation and De-Trending of Near-Infrared Diffuse Reflectance Spectra. Appl. Spectrosc. 43, 772–777. https://doi.org/10.1366/0003702894202201

Bartoli, F., 1983. The biogeochemical cycle of silicon in two temperate forest ecosystems. Ecol. Bull. 469–476.

Bertrand, I., Janik, L.J., Holloway, R.E., Armstrong, R.D., McLaughlin, M.J., 2002. The rapid assessment of concentrations and solid phase associations of macro-and micronutrients in alkaline soils by mid-infrared diffuse reflectance spectroscopy. Soil Res. 40, 1339–1356.

Blecker, S.W., McCulley, R.L., Chadwick, O.A., Kelly, E.F., 2006. Biologic cycling of silica across a grassland bioclimosequence: GRASSLAND SILICA CYCLING. Glob. Biogeochem. Cycles 20, n/a-n/a. https://doi.org/10.1029/2006GB002690

Boysworth, M.K., Booksh, K.S., 2008. Aspects of Multivariate Calibration Applied to Near-Infrared Spectroscopy, in: Handbook of Near-Infrared Analysis, Third Edition, PRACTICAL SPECTROSCOPY SERIES. pp. 207–229.

Brier, G.W., 1950. Verification of forecasts expressed in terms of probability. Mon. Weather Rev. 78, 1–3.

Brus, D.J., Saby, N.P.A., 2016. Approximating the variance of estimated means for systematic random sampling, illustrated with data of the French Soil Monitoring Network. Geoderma 279, 77–86.

Calaway, R., Corporation, M., Weston, S., Tenenbaum, D., 2017a. doParallel: Foreach Parallel Adaptor for the “parallel” Package.

Calaway, R., Microsoft Corporation, Weston, S., 2017b. foreach: Provides Foreach Looping Construct for R.

Carey, J.C., Fulweiler, R.W., 2012. The terrestrial silica pump. PLoS One 7, e52932.

Conley, D.J., Likens, G.E., Buso, D.C., Saccone, L., Bailey, S.W., Johnson, C.E., 2008. Deforestation causes increased dissolved silicate losses in the Hubbard Brook Experimental Forest. Glob. Change Biol. 14, 2548–2554.

Cornelis, J.-T., Ranger, J., Iserentant, A., Delvaux, B., 2010. Tree species impact the terrestrial cycle of silicon through various uptakes. Biogeochemistry 97, 231–245.

De Vos, W., Tarvainen, T., Salminen, R., Reeder, S., De Vivo, B., Demetriades, A., Pirc, S., Batista, M.J., Marsina, K., Ottesen, R.T., others, 2006. Geochemical Atlas of Europe:

Part 2: Interpretation of geochemical maps, additional tables, figures, maps, and related publications. Geological Survey of Finland.
Gneiting, T., Balabdaoui, F., Raftery, A.E., 2007. Probabilistic forecasts, calibration and sharpness. J. R. Stat. Soc. Ser. B Stat. Methodol. 69, 243–268.
Grinand, C., Barthès, B.G., Brunet, D., Kouakoua, E., Arrouays, D., Jolivet, C., Caria, G., Bernoux, M., 2012. Prediction of soil organic and inorganic carbon contents at a national scale (France) using mid-infrared reflectance spectroscopy (MIRS). Eur. J. Soil Sci. 63, 141–151. https://doi.org/10.1111/j.1365-2389.2012.01429.x
Hersbach, H., 2000. Decomposition of the Continuous Ranked Probability Score for Ensemble Prediction Systems. Weather Forecast. 15, 559–570. https://doi.org/10.1175/1520-0434(2000)015<0559:DOTCRP>2.0.CO;2
Imrie, C.E., Korre, A., Munoz-Melendez, G., Thornton, I., Durucan, S., 2008. Application of factorial kriging analysis to the FOREGS European topsoil geochemistry database. Sci. Total Environ. 393, 96–110. https://doi.org/10.1016/j.scitotenv.2007.12.012
James, G., Witten, D., Hastie, T., Tibshirani, R., 2013. An Introduction to Statistical Learning: with Applications in R. Springer Science & Business Media.
Janik, L., Skjemstand, J., Raven, M., 1995. Characterization and Analysis of Soils Using Midinfrared Partial Least-Squares .1. Correlations with Xrf-Determined Major-Element Composition. Aust. J. Soil Res. 33, 621–636. https://doi.org/10.1071/SR9950621
Janik, L.J., Skjemstad, J.O., Merry, R.H., 1998. Can mid infrared diffuse reflectance analysis replace soil extractions? Aust. J. Exp. Agric. 38, 681. https://doi.org/10.1071/EA97144
Jolivet, C., Arrouays, D., Boulonne, L., Ratié, C., Saby, N., 2006. Le réseau de mesures de la qualité des sols de France (RMQS). Etat D'avancement Prem. Résultats Etude Gest. Sols 13, 149–164.
Kuhn, M., Weston, S., Keefer, C., Coulter, N., 2016. Cubist: Rule- And Instance-Based Regression Modeling ; R package version 0.0.19. C code for Cubist by Ross Quinlan.
Laboratory NCAR-Research Applications, 2015. verification: Weather Forecast Verification Utilities.
Ligges, U., Short, T., Kienzle, P., Schnackenberg, S., Billinghurst, D., Borchers, H.-W., Carezia, A., Dupuis, P., Eaton, J.W., Farhi, E., Habel, K., Hornik, K., Krey, S., Lash, B., Leisch, F., Mersmann, O., Neis, P., Ruohio, J., III, J.O.S., Stewart, D., Weingessel, A., 2015. signal: Signal Processing.
Loucaides, S., Behrends, T., Van Cappellen, P., 2010. Reactivity of biogenic silica: Surface versus bulk charge density. Geochim. Cosmochim. Acta 74, 517–530.
Ma, J.F., Takahashi, E., 2002. Soil, fertilizer, and plant silicon research in Japan. Elsevier, Amsterdam.
McCarty, G.W., Reeves, J.B., Reeves, V.B., Follett, R.F., Kimble, J.M., 2002. Mid-infrared and near-infrared diffuse reflectance spectroscopy for soil carbon measurement. Soil Sci. Soc. Am. J. 66, 640–646.
Minasny, B., Hong, S.Y., Hartemink, A.E., Kim, Y.H., Kang, S.S., 2016. Soil pH increase under paddy in South Korea between 2000 and 2012. Agric. Ecosyst. Environ. 221, 205–213. https://doi.org/10.1016/j.agee.2016.01.042
Minasny, B., McBratney, A.B., 2008. Regression rules as a tool for predicting soil properties from infrared reflectance spectroscopy. Chemom. Intell. Lab. Syst. 94, 72–79.
Minasny, B., McBratney, A.B., 2006. A conditioned Latin hypercube method for sampling in the presence of ancillary information. Comput. Geosci. 32, 1378–1388. https://doi.org/10.1016/j.cageo.2005.12.009

Minasny, B., Tranter, G., McBratney, A.B., Brough, D.M., Murphy, B.W., 2009. Regional transferability of mid-infrared diffuse reflectance spectroscopic prediction for soil chemical properties. Geoderma 153, 155–162. https://doi.org/10.1016/j.geoderma.2009.07.021

Mohanty, B., Gupta, A., Das, B.S., 2016. Estimation of weathering indices using spectral reflectance over visible to mid-infrared region. Geoderma 266, 111–119. https://doi.org/10.1016/j.geoderma.2015.11.030

Monger, H.C., Kelly, E., 2002. Silica minerals, in: Soil Mineralogy with Environmental Applications., Soil Science Society of America Book Series. Soil Science Society of America Inc., Madison, Wisconsin, USA, pp. 611–636.

Morvan, X., Saby, N.P.A., Arrouays, D., Le Bas, C., Jones, R.J.A., Verheijen, F.G.A., Bellamy, P.H., Stephens, M., Kibblewhite, M.G., 2008. Soil monitoring in Europe: A review of existing systems and requirements for harmonisation. Sci. Total Environ. 391, 1–12. https://doi.org/10.1016/j.scitotenv.2007.10.046

Nguyen, T.T., Janik, L.J., Raupach, M., 1991. Diffuse reflectance infrared fourier transform (DRIFT) spectroscopy in soil studies. Soil Res. 29, 49–67. https://doi.org/10.1071/sr9910049

Quinlan, J.R., 1992. Learning with continuous classes, in: 5th Australian Joint Conference on Artificial Intelligence. Singapore, pp. 343–348.

R core Team, 2017. R: A Language and Environment for Statistical Computing. R Foundation for Statistical Computing, Vienna, Austria.

Reimann, C., Birke, M., Demetriades, A., Filzmoser, P., O'Connor, P., 2014. Chemistry of Europe's agricultural soils, part A.

Roudier, P., 2011. clhs: a R package for conditioned Latin hypercube sampling.

Savitzky, A., Golay, M.J., 1964. Smoothing and differentiation of data by simplified least squares procedures. Anal. Chem. 36, 1627–1639.

Soriano-Disla, J.M., Janik, L., McLaughlin, M.J., Forrester, S., Kirby, J., Reimann, C., 2013. The use of diffuse reflectance mid-infrared spectroscopy for the prediction of the concentration of chemical elements estimated by X-ray fluorescence in agricultural and grazing European soils. Appl. Geochem. 29, 135–143. https://doi.org/10.1016/j.apgeochem.2012.11.005

Soriano-Disla, J.M., Janik, L.J., Viscarra Rossel, R.A., Macdonald, L.M., McLaughlin, M.J., 2014. The Performance of Visible, Near-, and Mid-Infrared Reflectance Spectroscopy for Prediction of Soil Physical, Chemical, and Biological Properties. Appl. Spectrosc. Rev. 49, 139–186. https://doi.org/10.1080/05704928.2013.811081

Struyf, E., Smis, A., Van Damme, S., Garnier, J., Govers, G., Van Wesemael, B., Conley, D.J., Batelaan, O., Frot, E., Clymans, W., 2010. Historical land use change has lowered terrestrial silica mobilization. Nat. Commun. 1, 129.

Trinh, B.N., Thielen-del Pozo, J., Thirel, G., 2013. The reduction continuous rank probability score for evaluating discharge forecasts from hydrological ensemble prediction systems: Reduction continuous rank probability score for HEPS. Atmospheric Sci. Lett. 14, 61–65. https://doi.org/10.1002/asl2.417

Vaculikova, L., Plevova, E., 2005. Identification of clay minerals and micas in sedimentary rocks. Acta Geodyn. Geomater. 2, 163.

Van Looy, K., Bouma, J., Herbst, M., Koestel, J., Minasny, B., Mishra, U., Montzka, C., Nemes, A., Pachepsky, Y.A., Padarian, J., Schaap, M.G., Tóth, B., Verhoef, A., Vanderborght, J., van der Ploeg, M.J., Weihermüller, L., Zacharias, S., Zhang, Y., Vereecken, H., 2017. Pedotransfer Functions in Earth System Science: Challenges and Perspectives. Rev. Geophys. 2017RG000581. https://doi.org/10.1002/2017RG000581

Vandevenne, F., Struyf, E., Clymans, W., Meire, P., 2012. Agricultural silica harvest: have humans created a new loop in the global silica cycle? Front. Ecol. Environ. 10, 243–248.

Viscarra Rossel, R.A., Walvoort, D.J.J., McBratney, A.B., Janik, L.J., Skjemstad, J.O., 2006. Visible, near infrared, mid infrared or combined diffuse reflectance spectroscopy for simultaneous assessment of various soil properties. Geoderma 131, 59–75. https://doi.org/10.1016/j.geoderma.2005.03.007

Wedepohl, K.H., 1995. The composition of the continental crust. Geochim. Cosmochim. Acta 59, 1217–1232.

Wösten, J.H.M., Lilly, A., Nemes, A., Le Bas, C., 1999. Development and use of a database of hydraulic properties of European soils. Geoderma 90, 169–185. https://doi.org/10.1016/S0016-7061(98)00132-3

7- List of figures and tables:

Figures:

- Figure 1: Location of the sampling sites of the French monitoring network of soil quality (RMQS). Black triangles represent the sites for which Si measurements were available.
- Figure 2: Schematic diagram of the modelling procedure.
- Figure 3: Distribution of the Si concentrations in the Si dataset: a- histogram; b- boxplot. The dashed grey line represents the Si overall mean .
- Figure 4: Percentage of samples in different parent material classes for both the French monitoring network of soil quality (RMQS) database and the Si dataset.
- Figure 5: Comparison of the empirical density estimates of the pedological properties computed for all the sites (2088) of the French soil monitoring network (RMQS) and those of the Si dataset (673 sample).
- Figure 6: Principal component analysis of the whole dataset (2088 sampling sites) for two set of variables: Mid-infrared spectra (MIRS) (a and c) and pedological attributes (b and d). Bivariate plot of the scores of PCs 1 and 2 (a and b). Most correlated MIRS band are plotted in a. Score plot of first two components (c and d) (black points correspond to the extrapolated dataset from the French soil monitoring network (RMQS) and grey points to the Si dataset).
- Figure 7: Predicted versus measured Si concentrations (in g kg^{-1}) for the first cross validation replication of (a) the mid-infrared spectra (MIRS) and (b) the pedological pedotransfer Functions (PTFs). In black, the one to one line and in red, the fitted regression line. Black vertical error bars represent the prediction's uncertainty and blue horizontal error bars represent the analytical uncertainty.

562 - Figure 8: (a) Mid-infrared reflectance spectra (MIRS) of two sites randomly selected
563 among those with low Si concentrations (in grey) and high Si concentration (in black)
564 respectively; (b) average importance based on cubist models of spectral region for the
565 prediction of total Si concentration. Most important wavelengths (vertical lines) are
566 identified in Table 4.
567 - Figure 9: Average importance based on cubist model of the variables used for the
568 prediction of total Si concentration by pedological attributes.
569 - Figure 10: Scatterplot of the total Si concentration (in g kg^{-1}) predicted by the
570 pedological PedoTransfer Function (PTF) *versus* those predicted by the mid-infrared
571 spectra PTF. The samples correspond to the non-Si analysed sites of the French
572 monitoring network of soil quality (RMQS) (1407 sites).
573 - Figure 11: Empirical density estimate of Si concentrations obtained for the sites of the
574 French monitoring network of soil quality (RMQS) (this study) to those obtained for
575 French and European sites in GEMAS (Reimann et al., 2014). Vertical lines represent
576 the median values: 327.2 g kg^{-1}, 320.7 g kg^{-1} and 313.9 g kg^{-1} respectively.
577

Tables:

- Table 1 : Analytical methods employed for the selected soil properties
- Table 2: Summary statistics of pedological attributes for the two datasets: the RMQS and Si dataset.
- Table 3: Summary statistics of performance indicators of the cross-validation for the two PTF models. RMSE, bias and CRPS are in g kg^{-1}.
- Table 4: Important wavelengths in MIRS along with reported peaks and their assignments.

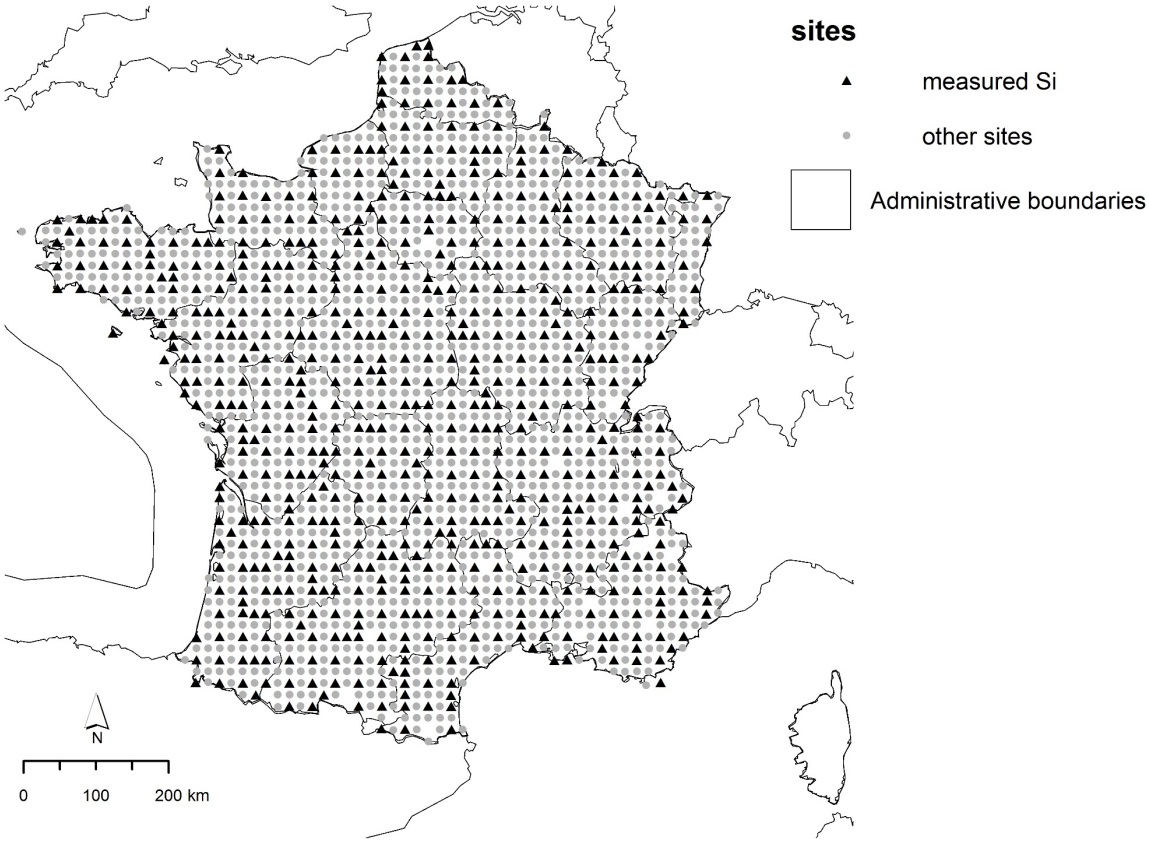

587
588 Figure 1
589

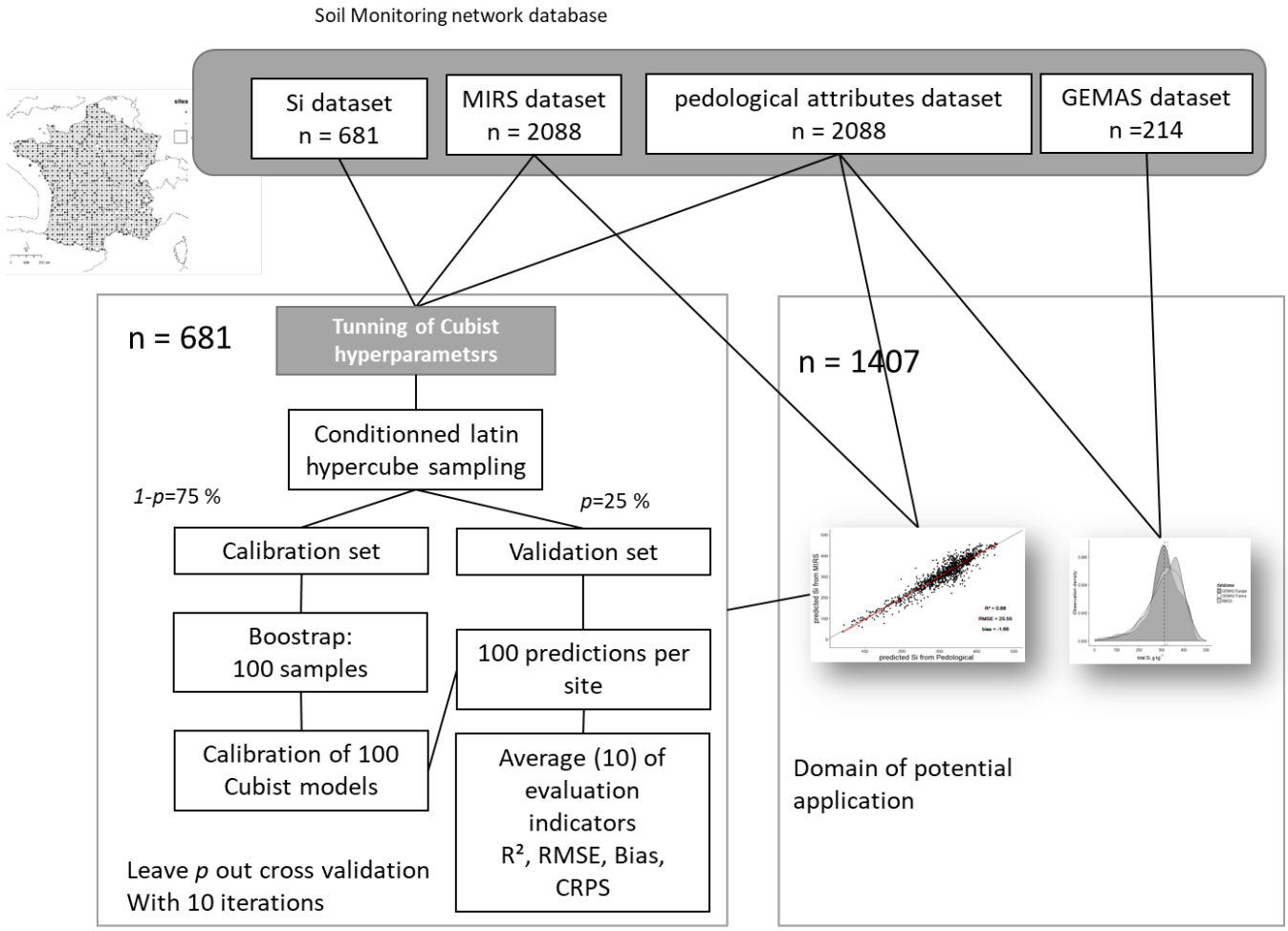
Soil Monitoring network database
Si dataset
n = 681
MIRS dataset
n = 2088
pedological attributes dataset
n = 2088
GEMAS dataset
n =214
n = 681
Tunning of Cubist hyperparametsrs
Conditionned latin hypercube sampling
1-p=75 %
p=25 %
Calibration set
Validation set
Boostrap:
100 samples
100 predictions per site
Calibration of 100 Cubist models
Average (10) of evaluation indicators
R², RMSE, Bias, CRPS
Leave p out cross validation
With 10 iterations
n = 1407
Domain of potential application

Figure 2

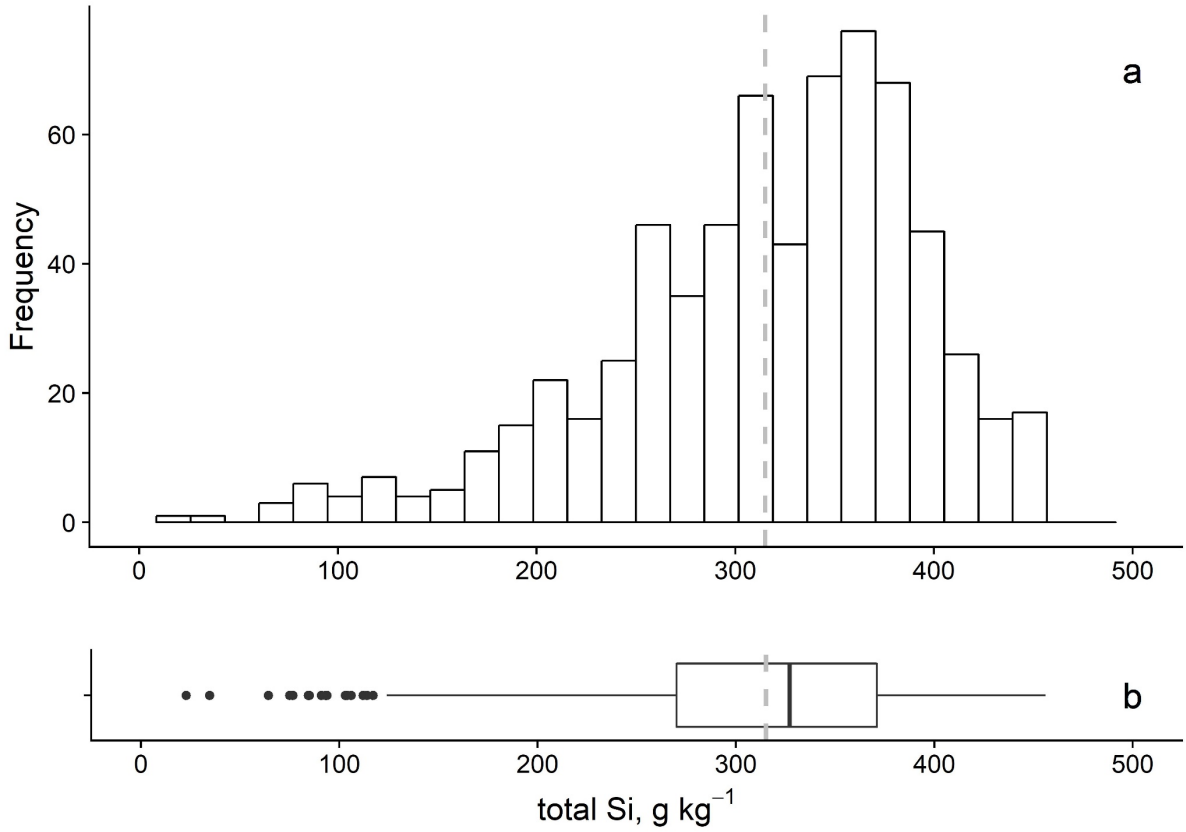

Figure 3

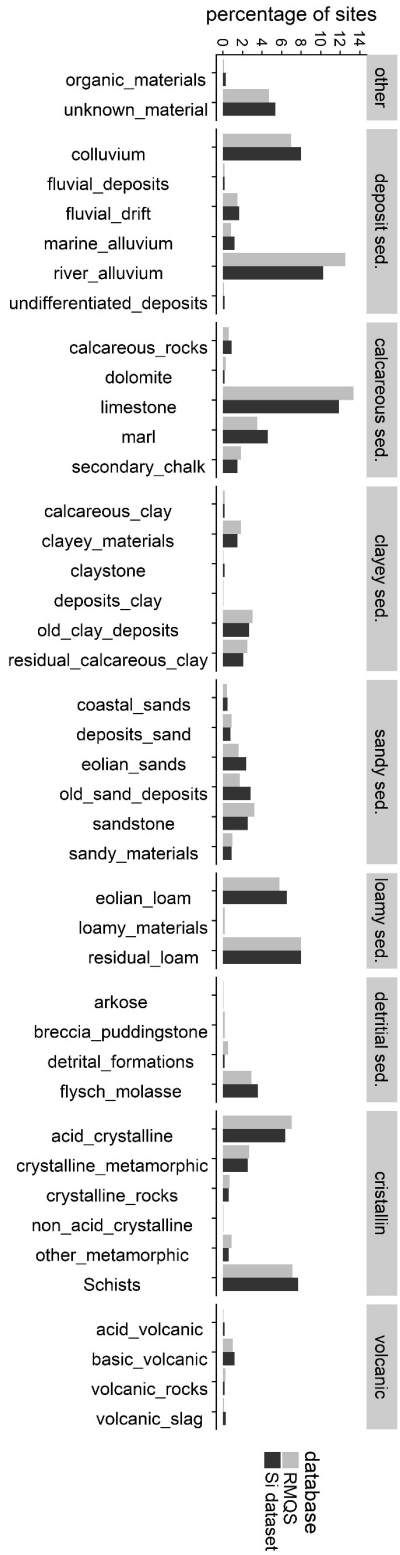

596
597 Figure 4
598

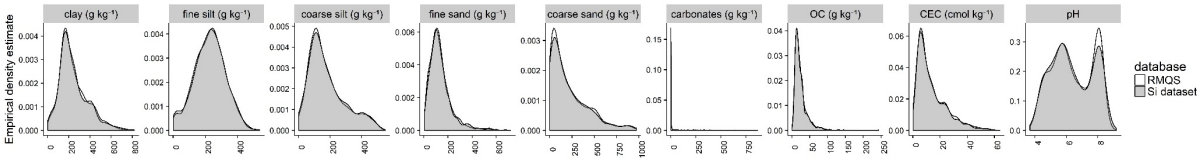

599
600 Figure 5

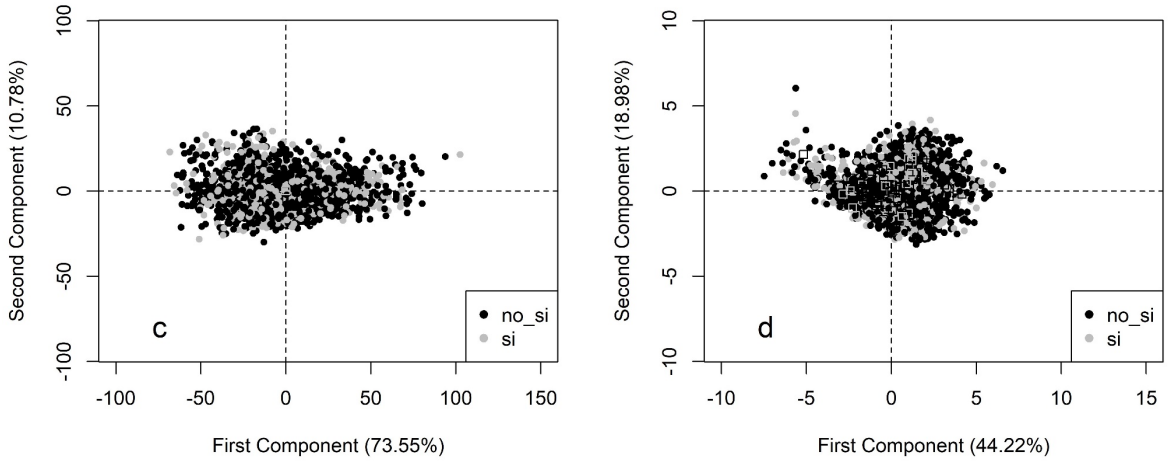

601
602 Figure 6
603

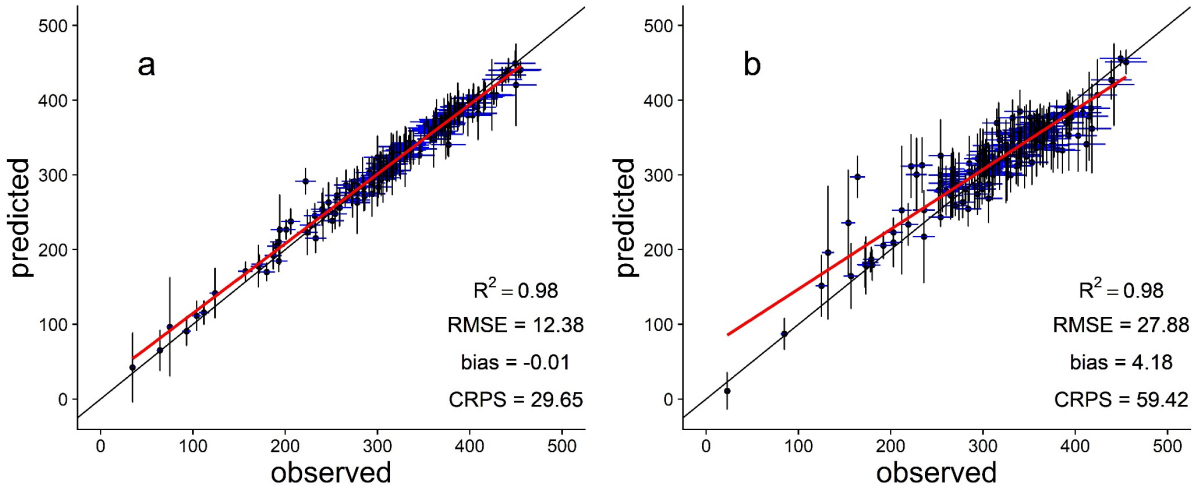

604
605 Fugure 7
606

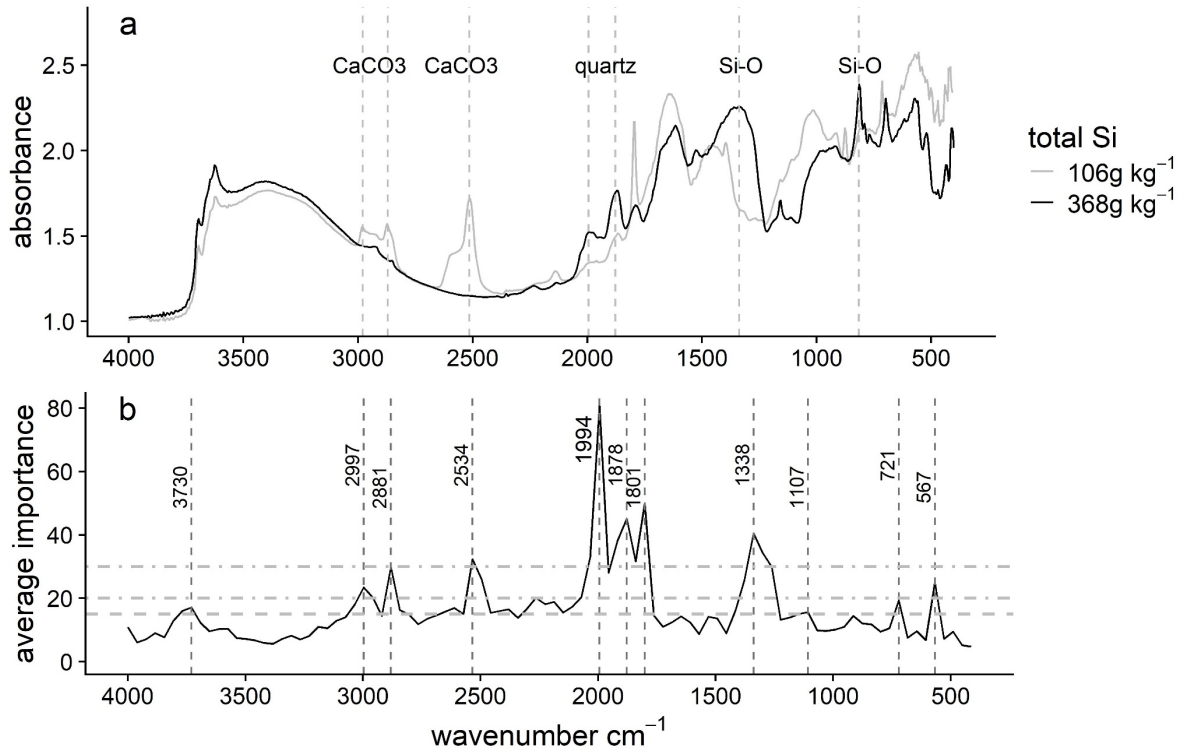

607
608 Figure 8

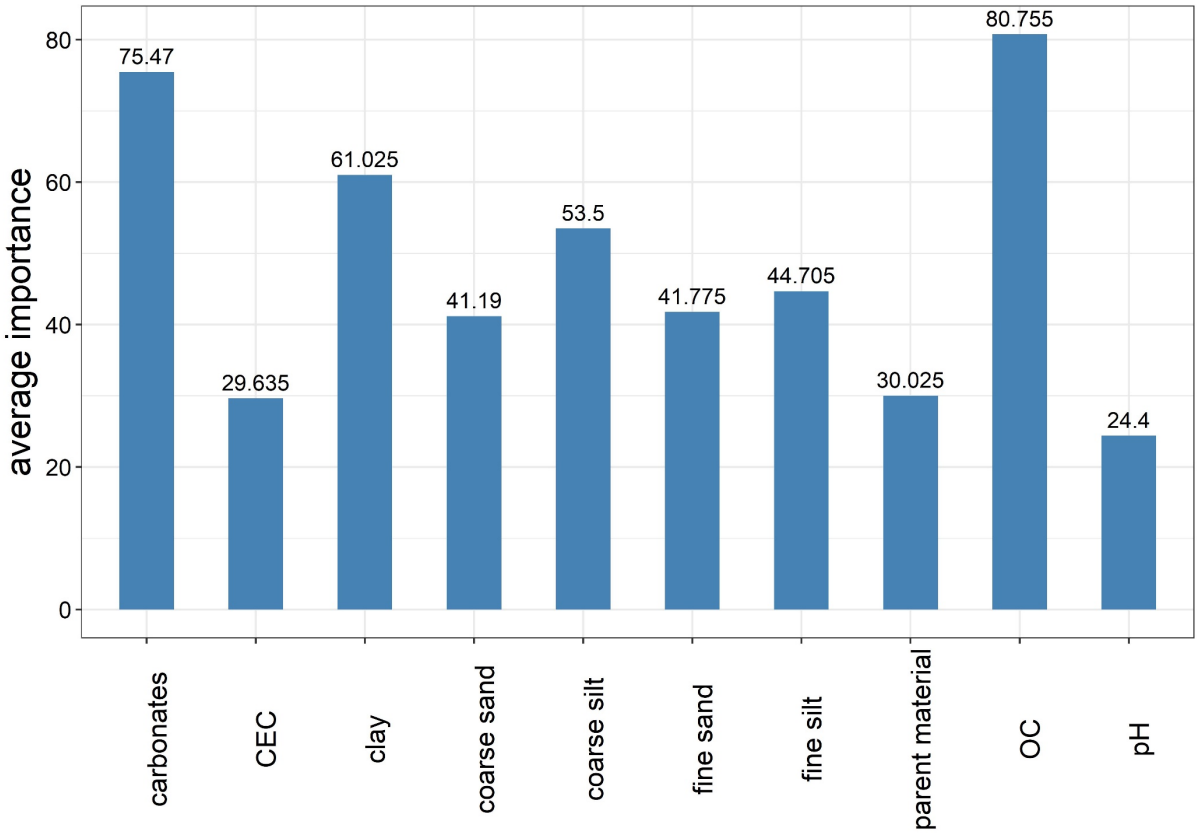

609
610 Figure 9
611

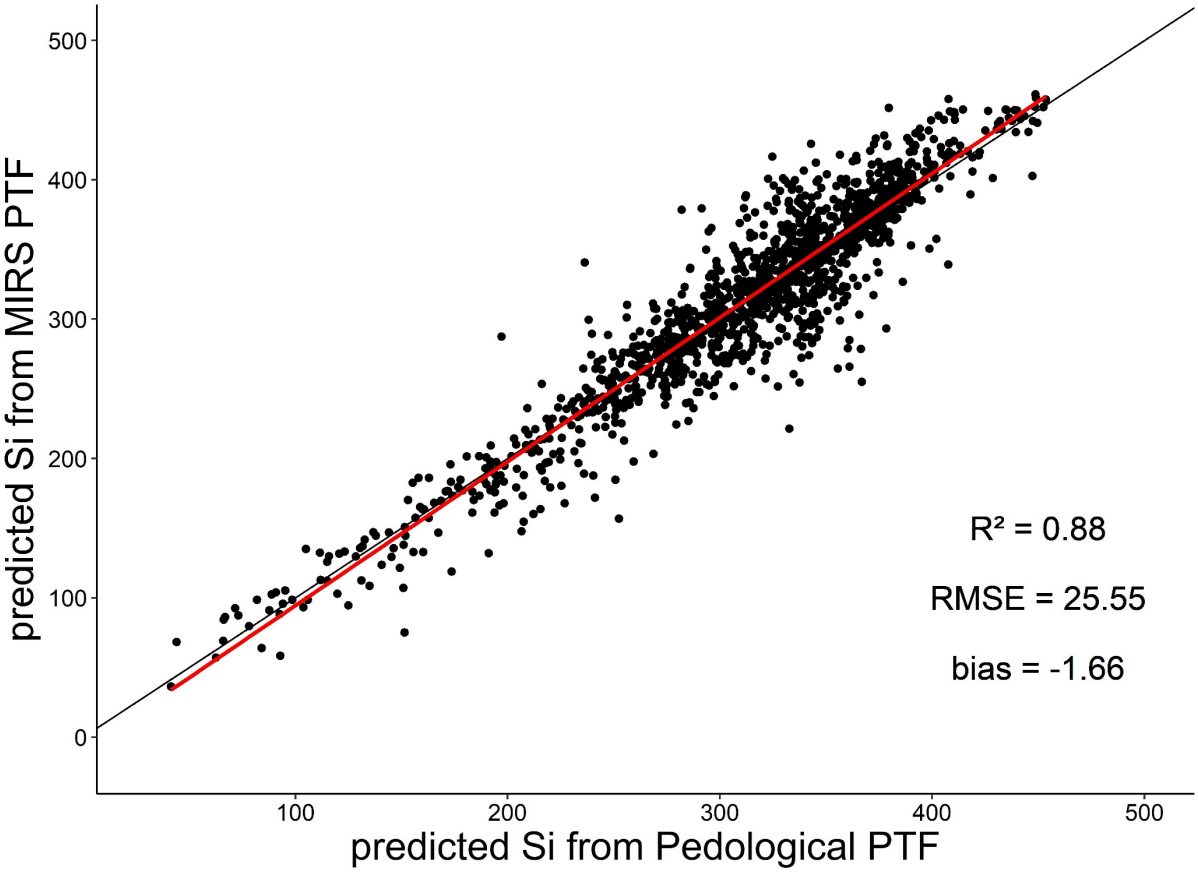

Figure 10

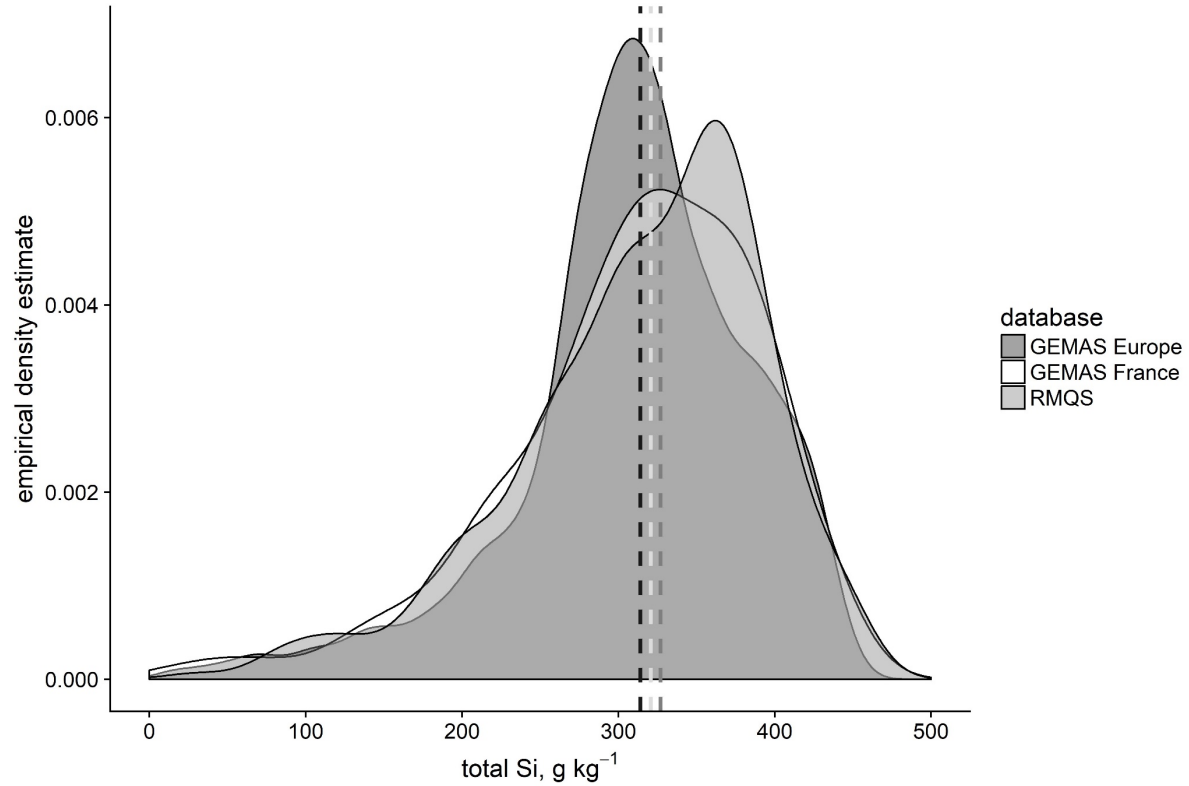

Figure 11

617 **Table 4 : Analytical methods employed for the selected soil properties**
618

Soil properties	Method	Source
Clay, fine silt, coarse silt, fine sand, coarse sand	Robinson's pipette after water sieving (NF X 31-107)	RMQS
CEC	Cobalthexammine extraction (NF X 31-130)	RMQS
pH	Water (ISO 10390)	RMQS
Organic carbon	Dry combustion (NF ISO 10694)	RMQS
Carbonates	Volumetric method (NF X 31-106)	RMQS
Total Si	ICP-AES after sodium peroxide fusion	This study
MIR Sectra	Diffusive Reflectance Fourier Transform Spectrophotometer from 4000 to 400 cm^{-1}	(Grinand et al., 2012)

619
620

621

Table 5: Summary statistics of pedological attributes for the two datasets: the RMQS and Si dataset. 622

Properties	Units	RMQS, n=2088		Si dataset, n=673		Wilcox-test p-value
		range	Median	range	Median	
Clay	g kg-¹	2 - 819	211	5 - 819	212	0.65
Fine silt	g kg-¹	1 - 539	231	1 - 539	231	0.99
Coarse silt	g kg-¹	1 - 551	146	1 - 518	144	0.81
Fine sand	g kg-¹	3 - 722	115	4 - 677	118	0.43
Coarse sand	g kg-¹	1 - 970	140	2 - 966	137	0.83
CEC	cmol kg-¹	0.3 - 64	10	0.5 - 60	10	0.36
pH	-	3.7 - 9.2	6.2	3.8 - 8.9	6.2	0.61
OC	g kg-¹	0.6 - 243	19.3	2.6 - 243	18.8	0.36
carbonates	g kg-¹	0.5 - 866	0.5	0.5 - 866	0.5	0.57

623
624

625 **Table 6: Summary statistics of performance indicators of the cross-validation for the two PTF models. RMSE, bias**
626 **and CRPS are in g kg⁻¹.**

Model	statistics	R^2	RMSE	Bias	CRPS
pedological	Min.	0.85	23.21	0.43	53.47
	Max.	0.90	28.57	5.63	64.88
	1st Qu.	0.86	25.50	1.19	55.62
	3rd Qu.	0.87	27.39	3.66	60.07
	Median	0.86	26.95	1.94	57.68
	Mean	0.87	26.48	2.37	58.04
	Var.	$0.2\ 10^{-3}$	2.47	3.12	13.16
	sd.	0.01	1.57	1.77	3.63
MIRS	Min.	0.94	11.41	-0.12	17.43
	Max.	0.98	17.67	3.71	29.65
	1st Qu.	0.95	14.21	0.20	19.74
	3rd Qu.	0.96	17.07	2.06	24.59
	Median	0.95	16.04	0.64	21.25
	Mean	0.96	15.31	1.15	22.36
	Var.	$0.2\ 10^{-3}$	4.70	1.57	14.32
	sd.	0.01	2.17	1.25	3.78

627
628
629

630 Table 7: Important wavelengths in MIRS along with reported peaks and their assignments.

631

Reported peaks (wavenumber in cm^{-1})	MIRS region from reference (wavenumber in cm^{-1})	Soil constituent and Assignment	Reference
567	600-150	clay : Si-O, Al-O bending	Vaculíková and Plevová, 2005
721	727-713	carbonates : CO_3	Vaculíková and Plevová, 2005; Nguyen et al., 1991
1107	1120-1000	clay : O-Si-O stretching	Saikia and Parthasarathy, 2010; Madejová, 2003
1300-1338	1360-1347	clay : Al-O as Si cage (TO_4)	Saikia and Parthasarathy, 2010
1801 1878 1994	2000-1650	quartz : O-Si-O stretching	Bertrand et al., 2002; Janik et al., 1998; Nguyen et al., 1991
2534	2600-2500	carbonates : $CaCO_3$ overtone and combinaison vibrations	D'Acqui et al., 2010; Du and Zhou, 2009; Vaculíková and Plevová, 2005; Bertrand et al., 2002; McCarty et al., 2002; Nguyen et al., 1991
2881	2880	carbonates : $CaCO_3$ overtone and combinaison vibrations	Vaculíková and Plevová, 2005; Bertrand et al., 2002; McCarty et al., 2002; Nguyen et al., 1991
2997	3000-2900	carbonates : $CaCO_3$ overtone and combinaison vibrations	Vaculíková and Plevová, 2005; McCarty et al., 2002; Nguyen et al., 1991
3730	3697 (1), 3750-3400 (2)	clay : Al---O-H stretching	Saikia and Parthasarathy, 2010 (1); Vaculíková and Plevová, 2005 (2); Nguyen et al., 1991

632

633